Modeling coupled thermal-hydrological-chemical processes in the unsaturated fractured rock of Yucca Mountain, Nevada: heterogeneity and seepage

S. Mukhopadhyay*, E.L. Sonnenthal, and N. Spycher
Lawrence Berkeley National Laboratory, Berkeley, CA 94720, USA

Abstract

An understanding of processes affecting seepage into emplacement tunnels is needed for correctly predicting the performance of underground radioactive waste repositories. It has been previously estimated that the capillary and vaporization barriers in the unsaturated fractured rock of Yucca Mountain are enough to prevent seepage under present day infiltration conditions. It has also been thought that a substantially elevated infiltration flux will be required to cause seepage after the thermal period is over. While coupled thermal-hydrological-chemical (THC) changes in Yucca Mountain host rock due to repository heating has been previously investigated, those THC models did not incorporate elements of the seepage model. In this paper, we combine the THC processes in unsaturated fractured rock with the processes affecting seepage. We observe that the THC processes alter the hydrological properties of the fractured rock through mineral precipitation and dissolution. We show that such alteration in the hydrological properties of the rock often leads to local flow channeling. We conclude that such local flow channeling may result in seepage under certain conditions, even with nonelevated infiltration fluxes.

Keywords: Seepage, THC Processes, Unsaturated zone, Yucca Mountain

1. Introduction

In the context of radioactive waste emplacement in an underground repository, *seepage* refers to flow of liquid water into the emplacement tunnels. Scientists have recently made substantial efforts towards understanding and predicting seepage in the unsaturated fractured rock of Yucca Mountain, Nevada. Both experimental and modeling analyses (Trautz and Wang, 2002; Finsterle et al., 2003) have been performed to determine the amount of seepage under ambient conditions, i.e., when no thermal effect is present. In addition, predictive modeling studies, based on stochastic continuum models, have been carried out to

* Corresponding author.
E-mail Addresses: Smukhopadhyay@lbl.gov (S. Mukhopadhyay), ELSonnenthal@lbl.gov (E.L. Sonnenthal), Nspycher@lbl.gov (N. Spycher)

predict the probability and magnitude of seepage under ambient conditions at Yucca Mountain (Tsang et al.,2004).

Those ambient seepage studies concluded that seepage under ambient conditions is prevented by the difference in the capillary pressure between the rock formation and a large underground opening (i.e., the emplacement tunnel), which is commonly referred to as the "capillary barrier." As a result, water is mostly diverted around the tunnels rather than flowing into them. Those previous investigations also concluded that the amount of ambient seepage, if any, is controlled by the magnitude of surface infiltration fluxes, the heterogeneities in the fracture permeability field, and the magnitude of the fracture capillary strength parameter (see below) of the host rock.

Heat generated by the emplaced radioactive waste causes the unsaturated rock at Yucca Mountain to stay above ambient temperatures for a long period of time. Thus, Birkholzer et al. (2004) investigated seepage during and after the thermal period at Yucca Mountain by simulating the thermal-hydrologic (TH) conditions in the unsaturated fractured rock surrounding the emplacement tunnels. Birkholzer et al. (2004) found that the quantity of seepage under thermal conditions is always smaller than ambient seepage, a result arising out of the presence of vaporization barrier (see Section 2), in addition to the capillary barrier. The other key finding from Birkholzer et al. (2004) is that the average percolation fluxes at Yucca Mountain are not sufficient to cause seepage into the emplacement tunnels. They further concluded that a substantially elevated background infiltration flux would be required to overcome the capillary and vaporization barriers at Yucca Mountain. While Birkholzer et al. (2004) estimated the transient pattern of seepage by analyzing the TH processes, the chemical changes in the host rock resulting from the elevated temperatures were not included in their conceptual model. It is our hypothesis that those chemical changes in the rock are pertinent for seepage. The objective of this paper is thus to investigate the combined effects of thermal-hydrological-chemical (THC) changes in hot, unsaturated fractured rock on seepage. Note that flow around an emplacement tunnel may also be influenced by coupled thermal-hydrological-mechanical (THM) processes as reported in Rutqvist and Tsang (2003) and Tsang et al. (2004), however, these THM models (similar to previous THC models) have not been explicitly coupled to the seepage models.

Seepage in heterogeneous fractured rock like that at Yucca Mountain is the result of two competing processes. The capillary forces of the fractured rock tend to prevent water from entering the emplacement tunnels. On the other hand, heterogeneity in the rock permeability leads to flow channeling in certain locations (zones of higher permeability) in preference to other locations (adjacent zones of lower permeability). If the flow channeling is so significant that the saturation builds up beyond a certain threshold, the capillary barrier is broken, and water begins to seep into the tunnels. Thus, heterogeneity in the hydrological properties of the rock plays a key role in influencing seepage.

For accurate prediction of seepage, two kinds of heterogeneities need to be considered in any conceptual model. The first type is the heterogeneity that is present in the rock before emplacement of wastes, i.e., the "ambient" or "geological" heterogeneities, resulting from physical and chemical changes occurring over geological time scales. All the previous ambient and thermal seepage analyses, including those of Birkholzer et al. (2004), considered only these ambient or geological heterogeneities. However, a second type of heterogeneity needs to be considered for accurate prediction of seepage. The elevated host rock temperatures, and subsequent moisture redistribution through boiling and condensation of pore water (see Section 2), cause varying spatial and temporal degrees of mineral precipitation and dissolution. These processes of precipitation and dissolution in turn change the hydrological properties (such as porosity, permeability, and even the capillary characteristics) of the rock, introducing additional chemical and hydrological heterogeneity in the rock. In the rest of the paper, we will show how these THC-induced "dynamic" heterogeneities lead to different transient patterns of seepage compared to seepage prediction excluding the chemical changes of the rock.

2. THC Processes

To understand the coupled THC processes arising from repository heating, we must first understand the associated TH processes. Heat conduction from the drift wall into the rock matrix results in vaporization and boiling, with vapor migration out of matrix blocks into fractures. The vapor moves away from the tunnel through the permeable fracture network by buoyancy, by the increased vapor pressure caused by

heating and boiling, and through local convection. In cooler regions, the vapor condenses on fracture walls, where it drains through the fracture network, either down toward the heat source from above or away from the drift into the zone underlying the heat source. Slow imbibition of water from fractures into the matrix gradually leads to increases in the liquid saturation of the rock matrix. Under conditions of continuous heating, a *dryout* zone (Figure 1) may develop closest to the heat source, separated from the condensation zone by a nearly isothermal zone maintained at about the boiling temperature. This nearly isothermal zone is characterized by a continuous process of boiling, vapor transport, condensation, and migration of water back to the heat source, and is often termed a *heat pipe* (Pruess et al., 1990). The dryout zone, by exposing any incoming water to vigorous boiling, retards and reduces the flow of water towards the emplacement tunnel. It is thus often called a *vaporization barrier* (Birkholzer et al., 2004).

The chemical evolution of waters, gases, and minerals is intimately coupled to the TH processes discussed above. The distribution of condensate in the fracture system determines where mineral dissolution and precipitation can occur in the fractures and where direct interaction (via diffusion) can occur between matrix pore waters and fracture waters. Figure 1 schematically shows the relationships between TH and chemical processes in the zones of boiling, condensation, and drainage in the rock mass, at the fracture-matrix interface outside of the emplacement tunnel and above the heat source. Zonation in the distribution of mineral phases can occur as a result of differences in mineral solubility as a function of temperature. The inverse relation between temperature and calcite solubility (as opposed to the silica phases, which are more soluble at higher temperatures) can cause zonation in the distribution of calcite and silica phases in both the condensation and boiling zones.

Spycher et al. (2003) discuss the main mineral precipitation and dissolution reactions expected to occur because of repository heating. Summarizing, amorphous silica precipitates from boiling and evaporation, and calcite by heating and CO_2 volatilization (i.e., $Ca^{2+} + 2HCO_3^- \Rightarrow CaCO_{3(s)} + CO_{2(g)}\uparrow + H_2O$). The precipitation of amorphous silica, and to a much lesser extent calcite, is the main cause of long-term permeability reduction. Evaporative concentration also results in the precipitation of gypsum (or anhydrite), halite, fluorite and other salts. These evaporite minerals eventually redissolve during the

collapse of the boiling front, however, their precipitation results in a significant temporary decrease in permeability (see Figure 5). Clays and zeolites (predominantly stellerite) also precipitate in small quantities without significant effect on permeability. These minerals form mostly in the rock matrix as the alteration product of rock-forming feldspars (e.g., $2.33NaAlSi_3O_8$ [albite] + $2H^+$ ==> $Na_{0.33}Al_{2.33}Si_{3.67}O_{10}(OH)_2$ [smectite] + $3.32SiO_2$ + $2Na^+$; $2\ NaAlSi_3O_8$ [albite] + SiO_2 + $CaCO_3$ [calcite] + H^+ + $7H_2O$ <==> $CaAl_2Si_7O_{18} \bullet 7H_2O$ [stellerite] + $2Na^+$ + HCO_3^-). Therefore, precipitation of amorphous silica or another silica phase is likely to be confined to a narrower zone where evaporative concentration from boiling occurs. In contrast, calcite precipitates in fractures over a broader zone of elevated temperature and where CO_2 has exsolved because of temperature increase or boiling.

3. Modeling Approach

Models have recently been developed to investigate the THC processes at Yucca Mountain (Sonnenthal et al., 2005; Spycher et al., 2003; Spycher et al., 2005). Similar to those THC models, the THC Seepage Model in this paper is based on the non-isothermal reactive geochemical transport software, TOUGHREACT (Xu et al., 2001 and 2004). TH processes simulated with the TOUGHREACT software are equivalent to those in TOUGH2 (Pruess et al., 1999). The geochemical module incorporated in TOUGHREACT simultaneously solves a set of chemical mass-action, kinetic-rate expressions for mineral dissolution/precipitation and mass-balance equations. Equations for heat, liquid, and gas flow, aqueous and gaseous species transport, and chemical reactions are provided in Xu et al. (2004). Thermodynamic data (including stability constants) as functions of temperature are read from a database created mostly using SUPCRT92 (Johnson et al., 1992), with modifications described in Spycher et al. (2005). Some uncertainties in these thermodynamic data, particularly at higher temperatures, may exist; however, testing of the THC seepage model with THC data from large-scale field heater tests provides confidence in the model results (see Section 4). A complete discussion of the modeling approach adopted in this paper can be found in Spycher et al. (2006). For the sake of completeness, a summary of the modeling approach is provided below.

In the THC Seepage Model, the unsaturated fractured rock of Yucca Mountain is conceptualized as dual permeability (Pruess, 1991), where the rock matrix and the embedded fractures are modeled as two separate but interacting continua. Because only a subset of all fractures may be actively contributing to the flow processes, an "active fracture" version (Liu et al., 1998) of the classical dual permeability model is used in this paper.

Note that, with respect to flow channeling and the effectiveness of the capillary barrier for seepage into tunnels, a two-dimensional (2-D) representation increases the potential for seepage in most cases of heterogeneous fracture permeability fields because the potential diversion of flow in the third dimension is neglected (Birkholzer et al., 2004). Therefore, TH and THC simulations in this paper were performed in a 2-D vertical cross section, extending from the ground surface at the top to the water table at the bottom. Laterally, the model domain extends from the center of one emplacement tunnel to the mid-point between two adjacent tunnels, which is treated as a vertical no-flow boundary. Symmetry is assumed with the symmetry plane parallel to the drift axis. The grid is radial and refined in the vicinity of the emplacement tunnel, however, it is coarser farther from the tunnel and gradually transforms into a rectangular grid (see Figure 2). Both the top and the bottom boundaries are assigned Dirichlet-type conditions with fixed temperature, pressure, and liquid saturation values. The top boundary is treated as an open atmosphere with constant CO_2 partial pressure and fixed composition of the infiltrating water. The groundwater table at the bottom of the model is represented as a flat, stable surface saturated with water and CO_2 partial pressure at equilibrium. The lateral boundaries are no-flow boundaries for flow, heat, and chemical fluxes. Infiltration fluxes of 6, 16, and 25 mm/year, are applied at the top model boundary during 0-600, 600-2,000, and beyond 2,000 years, respectively, consistent with future climate analysis at Yucca Mountain (Houseworth, 2001). These same infiltration fluxes have been used in previous thermal seepage studies (Birkholzer et al., 2004). Note that a revised analysis of the future climate at Yucca Mountain has been recently developed (Campbell et al., 2004), however, the actual percolation fluxes used in this paper are obtained from Houseworth (2001).

The thermal load imposed on the THC Seepage Model is identical to previous modeling studies (Birkholzer et al., 2004; Spycher et al., 2005). Hydrological and thermal properties for the matrix and fracture continua of the various geological units in the model domain are obtained from Ghezzehei and Liu (2004). For the THC simulations, the mineralogical data, and the initial water and gas composition data, are obtained from Spycher et al. (2005). One key parameter controlling seepage under both ambient and thermal conditions is the effective fracture capillary strength parameter ($1/\alpha$) of the host rock. The fracture $1/\alpha$ of the host rock (=589 Pa) used in this paper is obtained from ambient liquid-release testing at Yucca Mountain (Finsterle et al., 2003). Note that, even though the THC processes are expected to dynamically alter the fracture $1/\alpha$ parameter, this effect has not been included in this paper. It is possible that, when the effect of mineral precipitation and dissolution on fracture capillarity is included in the model (such as through Leverett scaling), seepage scenarios may emerge that are different from those presented in this paper. A qualitative discussion on this matter can be found in Spycher et al. (2006) and analysis is currently underway to investigate this issue more quantitatively.

The emplacement tunnels at Yucca Mountain will be located mostly in the lower lithophysal (Tptpll or tsw35) unit of the Topopah Spring fractured tuff. Measured fracture permeability data in Tptpll show a four-order-of-magnitude variability in space, and the arithmetic average of standard deviation in log10 space of all air-permeability measurements is 0.91 (Tsang et al.,, 2004). A log-normal fracture permeability distribution is thus developed with a standard deviation of 1.0 in the log10 space, consistent with previous seepage studies (Tsang et al., 2004). The mean fracture permeability of various stratigraphic units is obtained from Ghezzehei and Liu (2004). Three realizations of the heterogeneous fracture permeability fields were generated, each of which was based on the same cumulative distribution function (Tsang et al., 2004), but with a different seed number for the random number generator.

4. Model Testing

The modeling framework of the THC Seepage Model was tested using data from large-scale *in situ* heater experiments at Yucca Mountain (Spycher et al., 2003). This validates the THC Seepage Model with respect to the effects from coupled THC processes on chemical conditions represented by water and gas

compositions. The two most important rock parameters for seepage are heterogeneity in the fracture permeability distribution, and fracture $1/\alpha$. In the THC Seepage Model, the heterogeneous fracture permeability distribution is generated based on calibrated air-permeability measurement data. The fracture $1/\alpha$ of the Tptpll, unit on the other hand, was obtained from calibration of seepage data from ambient liquid release tests. Note that the THC Seepage Model cannot be tested for seepage directly because the heater tests at Yucca Mountain did not produce seepage. The results presented in this paper are scooping in nature and demonstrate the coupling between THC processes and seepage, that is implied by integration of the available in situ testing data from ambient temperatures and heater tests.

5. Results

Contours of fracture liquid saturation and temperature, and the liquid flux vectors at 2,000 years for TH and THC simulations are shown in Figure 3. While flow is diverted around the emplacement tunnel in Figure 3a without any channeling on the tunnel wall, significant local flow channeling is seen on the tunnel wall in Figure 3b. Figure 3b also shows that liquid water actually enters the tunnel (i.e., seepage is taking place), whereas no such seepage phenomenon is seen in Figure 3a.

The channeling of flow (and subsequent seepage) in Figure 3b is the result of THC processes altering the hydrological properties of the host rock. This can be clearly seen from Figure 4, where contours of fracture permeability from THC simulations are presented at 600 (Figure 4a) and 2,000 years (Figure 4b). Observe that an "umbrella" of highly reduced permeability above the tunnel is formed at 600 years (Figure 4a). After 600 years, because of enhanced infiltration fluxes from climate changes, dissolution of the mineral precipitates accelerates. With continued dissolution of the precipitates, the umbrella of reduced permeability moves nearer to the tunnels. Specific to this particular simulation, the umbrella of reduced permeability is situated on the wall of the emplacement tunnel between 1,600 years and 2,000 years (Figure 4b). After 2,000 years, further increase in the infiltration fluxes caused by another change in climate causes even faster dissolution of the precipitates, and the fracture permeability field close to the tunnel is almost restored to ambient conditions (not shown here).

The channeling of flow in Figure 3b is thus related to the pattern of fracture permeability in the grid blocks (of Figure 2) just above the tunnels. For example, fracture permeabilities in the twelve grid blocks just above the tunnel at various times from THC simulations are shown in Figure 5 as a function of their radial location with respect to the vertical. Observe the sudden decrease in permeability in almost all the gridblocks (except those close to the springline or 90^o) at around 1,600 years, and the increase in their values after 2,000 years. Observe also that the two gridblocks located at 33.75^o and 41.25^o are flanked by gridblocks whose permeabilities are a few orders of magnitude smaller than those two during that time. Comparing with Figure 3b, flow is seen to be channeleded on those locations only; these are the locations through which seepage happens. Thus, the THC processes introduce additional heterogeneities (not seen in TH-only simulations) in the fracture hydrological properties, which result in seepage.

TH-only simulations with any of the three realizations of the fracture permeability distributions do not predict any seepage. The amount of seepage from THC simulations using the three realizations of the fracture permeability distribution is shown in Figure 6. Figure 6 also shows the infiltration fluxes at different times during the simulation. Observe that the transient pattern of seepage is similar for two of the three realizations, with a maximum predicted seepage rate of 10-12 mm/year at around 1,600 years. However, the amount of seepage is almost nonexistent in the third realization. Figure 6 shows that THC processes introduce enough spatial variability in hydrological properties on the background heterogeneous permeability field to cause seepage for two of the three realizations. However, insignificant seepage occurs for the third realization. This finding illustrates the importance of both the background (or geological) heterogeneity and the THC-induced heterogeneities in controlling seepage. In summary, whether seepage happens or not is determined by the local heterogeneity in fracture hydraulic properties, and the THC processes influence seepage by dynamically altering these hydraulic properties.

6. Conclusions

Heat emanating from emplaced radioactive wastes cause coupled THC changes in the rock hosting the repository. These THC changes include the processes of mineral precipitation and dissolution, which in turn change the hydrologic properties of the rock, particularly the porosity and permeability. We model the THC processes around an emplacement tunnel in the unsaturated fractured rock of Yucca Mountain and

show that these processes introduce additional heterogeneity in the host rock. We demonstrate that these THC-induced heterogeneities in an already heterogeneous fracture permeability field cause local flow channeling. We establish that such local flow channeling may lead to seepage even when the infiltration fluxes are nonelevated. We perform THC simulations with three realizations of the fracture permeability field, and determine the pattern of transient seepage including the maximum rate of seepage. Simulations with many more realizations of the fracture permeability distribution may be needed to determine the average rate of seepage. However, the results presented here sufficiently demonstrate the role of heterogeneity on seepage under THC conditions.

Acknowledgments

This work was supported by the Director, Office of Civilian Radioactive Waste Management, U.S. Department of Energy, through Memorandum Purchase Order EA9013MC5X between Bechtel SAIC Company, LLC, and the Ernest Orlando Lawrence Berkeley National Laboratory (Berkeley Lab). The support is provided to Berkeley Lab through the U.S. Department of Energy Contract No. DE-AC03-76SF00098. Review and comments from Tianfu Xu and Dan Hawkes of the Berkeley Lab are greatly appreciated.

References

Birkholzer, J.T., Mukhopadhyay, S., and Tsang, Y.W., 2004. Modeling seepage into heated waste emplacement tunnels in unsaturated fractured rock. Vadose Zone Journal, 3, 819-836.

Campbell, C.G., Levitt, D., and Bakr, A., Future Climate Analysis, ANL-NBS-GS-000008 REV 01. Bechtel SAIC Company, Las Vegas, NV.

Finsterle, S., Ahlers, C.F., Trautz, R.C., and Cook, P.J., 2003. Inverse and predictive modeling of seepage into underground openings. Journal of Contaminant Hydrology, 62–63, 89-109.

Ghezzehei, T.A. and Liu, H.H., 2004. Calibrated Properties Model, MDL-NBS-HS-000003 REV 02. Bechtel SAIC Company, Las Vegas, NV.

Houseworth, J., 2001. Future climate analysis, ANL-NBS-GS-000008 REV00 ICN 01. USGS, Denver, CO.

Johnson, J.W., Oelkers, E.H., and Helgeson, H.C., 1992. SUPCRT92: A software package for calculating the standard molal thermodynamic properties of minerals, gases, aqueous species, and reactions from 1 to 5000 bars and 0 to 1000 degrees C. *Computers and Geosciences*, 18, 899–948.

Liu, H.H., Doughty, C., and Bodvarsson, G.S., 1998. An active fracture model for unsaturated flow and transport in fracture rocks. Water Resources Research, 34(10), 2633–2646.

Pruess, K., 1991. TOUGH2 — A general purpose numerical simulator for multiphase fluid and heat flow, LBNL-29400. Lawrence Berkeley National Laboratory, Berkeley, CA.

Pruess, K., Wang, J.S.Y., and Tsang, Y.W., 1990. On thermohydrologic conditions near high-level nuclear wastes emplaced in partially saturated fractured tuff, 1. Simulation studies with explicit consideration of fracture effects. Water Resources Research, 26(6), 1235–1248.

Pruess, K., Oldenburg, C.M., and Moridis, G., 1999. TOUGH2 user's guide, Version 2.0, LBNL-43134. Lawrence Berkeley National Laboratory, Berkeley, CA.

Rutqvist, J. and Tsang, C.F., 2003. Analysis of thermal-hydrological-mechanical behavior near an emplacement drift at Yucca Mountain. Journal of Contaminant Hydrology, 62-63, 637-652.

Sonnenthal, E. L., Ito, A., Spycher, N., Yui, M., Apps, J., Sugita, Y., Conrad, M., and Kawakami, S., 2005. Approaches to modeling coupled thermal, hydrological, and chemical processes in the Drift Scale Heater Test at Yucca Mountain. International Journal of Rock Mechanics and Mining Sciences, 42, 698-719.

Spycher, N., Sonnenthal, E.L., and Apps, J., 2003. Prediction of fluid flow and reactive transport around potential nuclear waste emplacement tunnels at Yucca Mountain, Nevada. Journal of Contaminant Hydrology, 62-63, 653–673.

Spycher, N., Sonnenthal, E.L., and Bryan, C., 2005. Drift-scale THC seepage model, MDL-NBS-HS-000001 REV 04. Bechtel SAIC Company, Las Vegas, NV.

Spycher, N., Mukhopadhyay, S., Shileds, D., Leem, J., Bryan, C., and Sonnenthal, E.L., 2006. THC sensitivity study of repository edge and heterogeneous permeability effects, ANL-NBS-HS-000047 REV 00. Bechtel SAIC Company, Las Vegas, NV.

Trautz, R.C. and Wang, J.S.Y., 2002. Seepage into am underground opening constructed in unsaturated fractured rock under evaporative conditions. Water Resources Research, 38(10), 6-1 through 6-14, 2002.

Tsang, C.F., Li, G., Rutqvist, J., and Zhou, Q., 2004. Seepage Model for PA Including Drift Collapse, MDL-NBS-HS-000002 REV 03. Bechtel SAIC Company, Las Vegas, NV.

Xu, T., Sonnenthal, E.L., Spycher, N., Pruess, K., Brimhall, G., and Apps, J., 2001. Modeling multiphase fluid flow and reactive geochemical transport in variably saturated fractured rocks: 2. Applications to supergene copper enrichment and hydrothermal flows. American Journal of Science, 301, 34-59.

Xu, T., Sonnenthal, E.L., Spycher, N., and Pruess, K., 2004. TOUGHREACT user's guide: A simulation program for non-isothermal multiphase reactive geochemical transport in variable saturated geologic media, Report LBNL-55460. Lawrence Berkeley National Laboratory, Berkeley, CA.

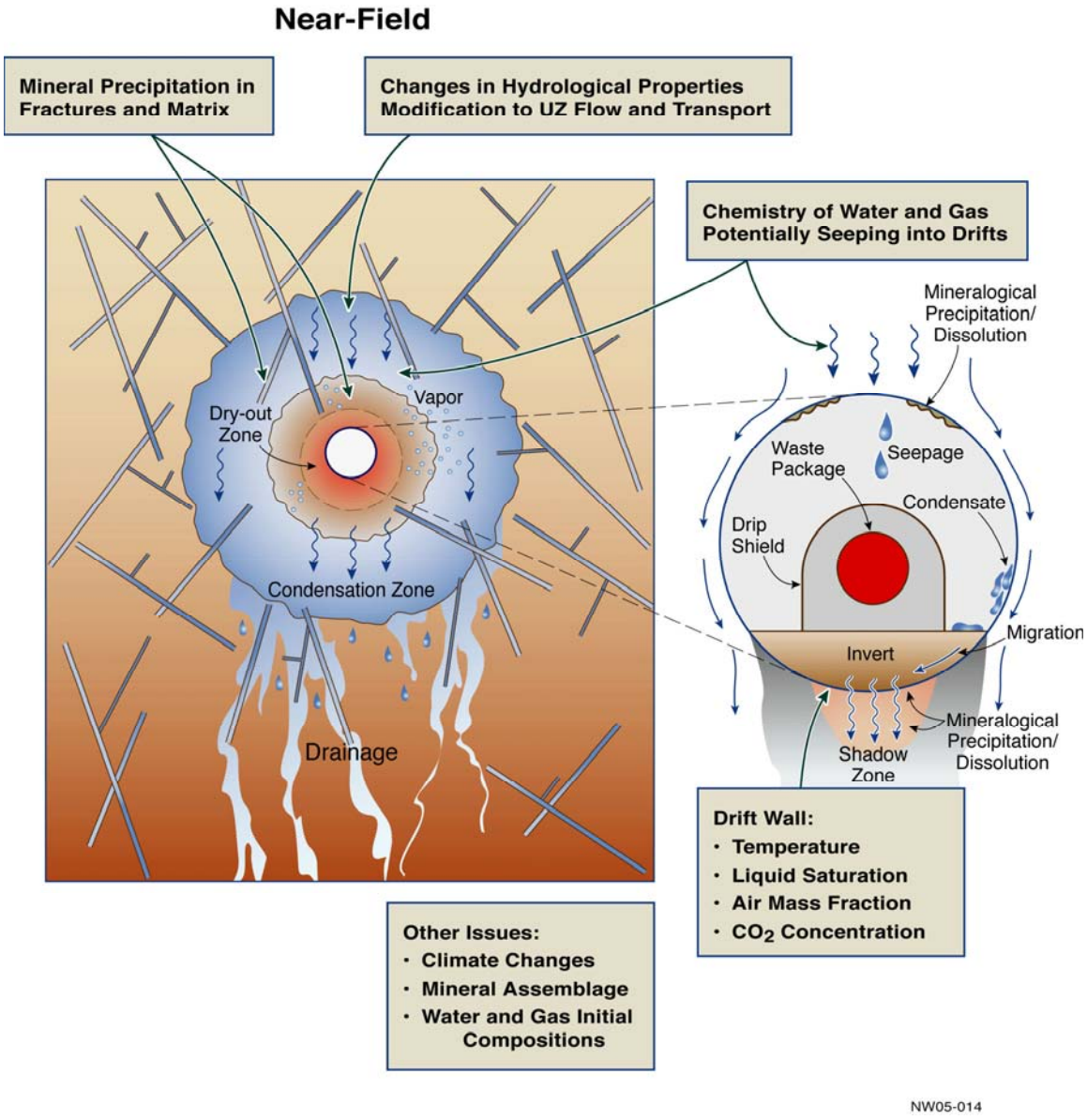

Figure 1. Schematic representation of TH and THC processes in the unsaturated zone (UZ) around an emplacement tunnel.

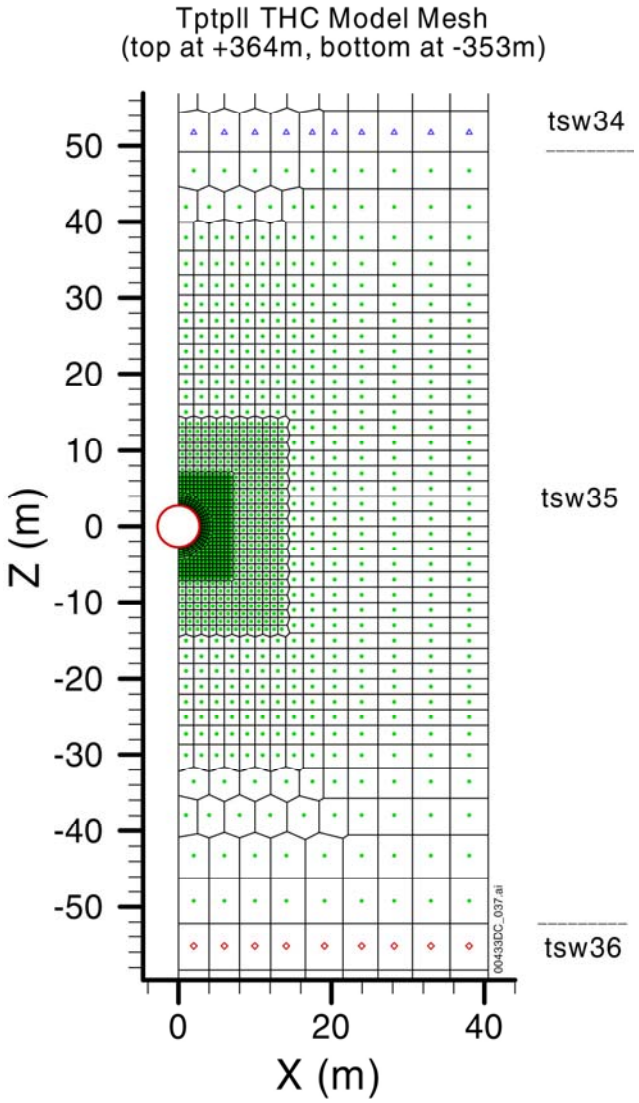

Figure 2: The 2-D THC seepage model domain near an emplacement tunnel. The tunnel is located in the lower lithophysal (tsw35) unit of Topopah Spring Tuff (Tpt) at Yucca Mountain. The overlying unit is the upper nonlithophysal (tsw34) zone and the underlying unit is the lower nonlithophysal (tsw36) of Tpt.

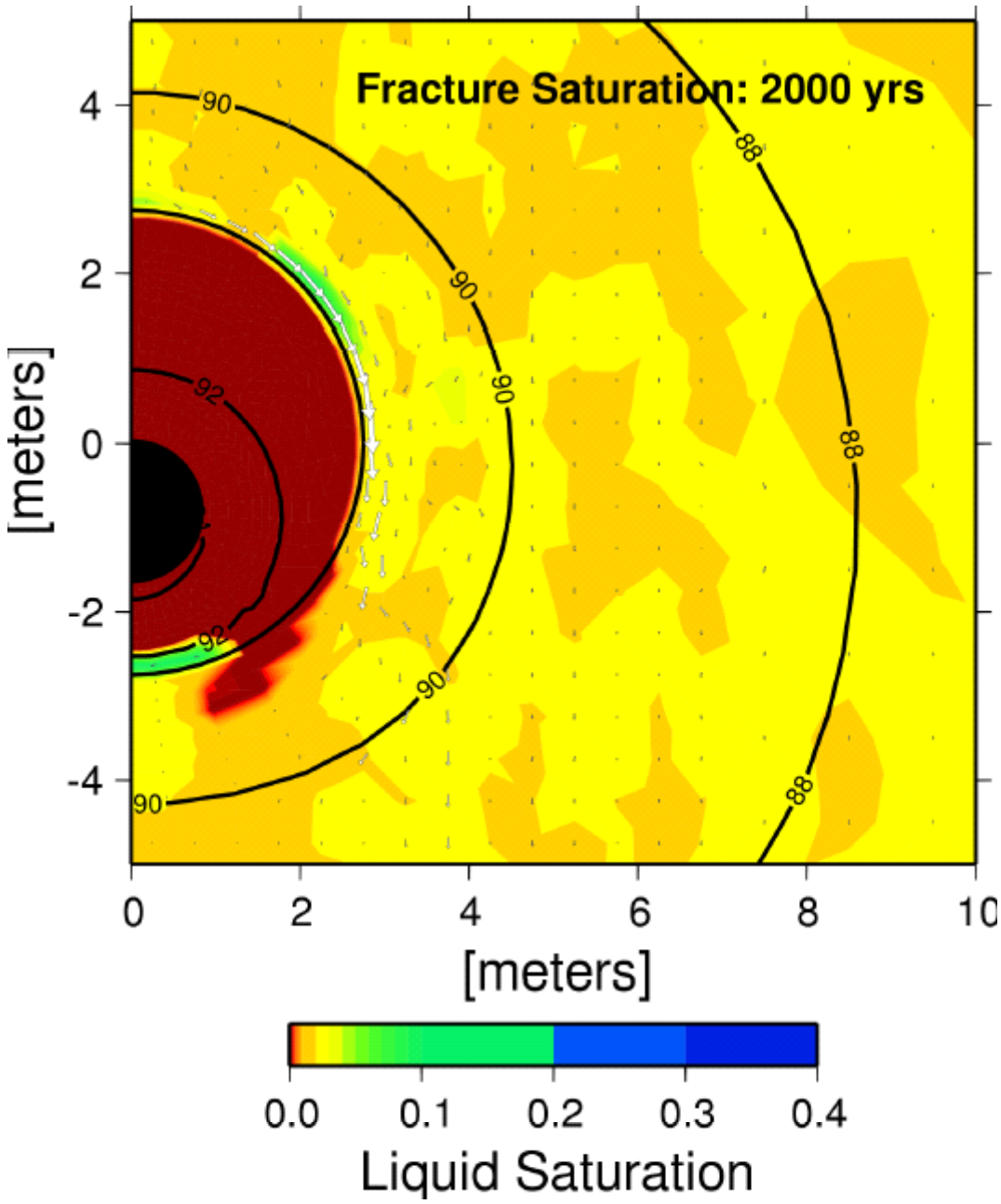

Figure 3a. Contours of saturation and temperature (solid lines), and liquid flux vectors in TH-only simulations at 2,000 years

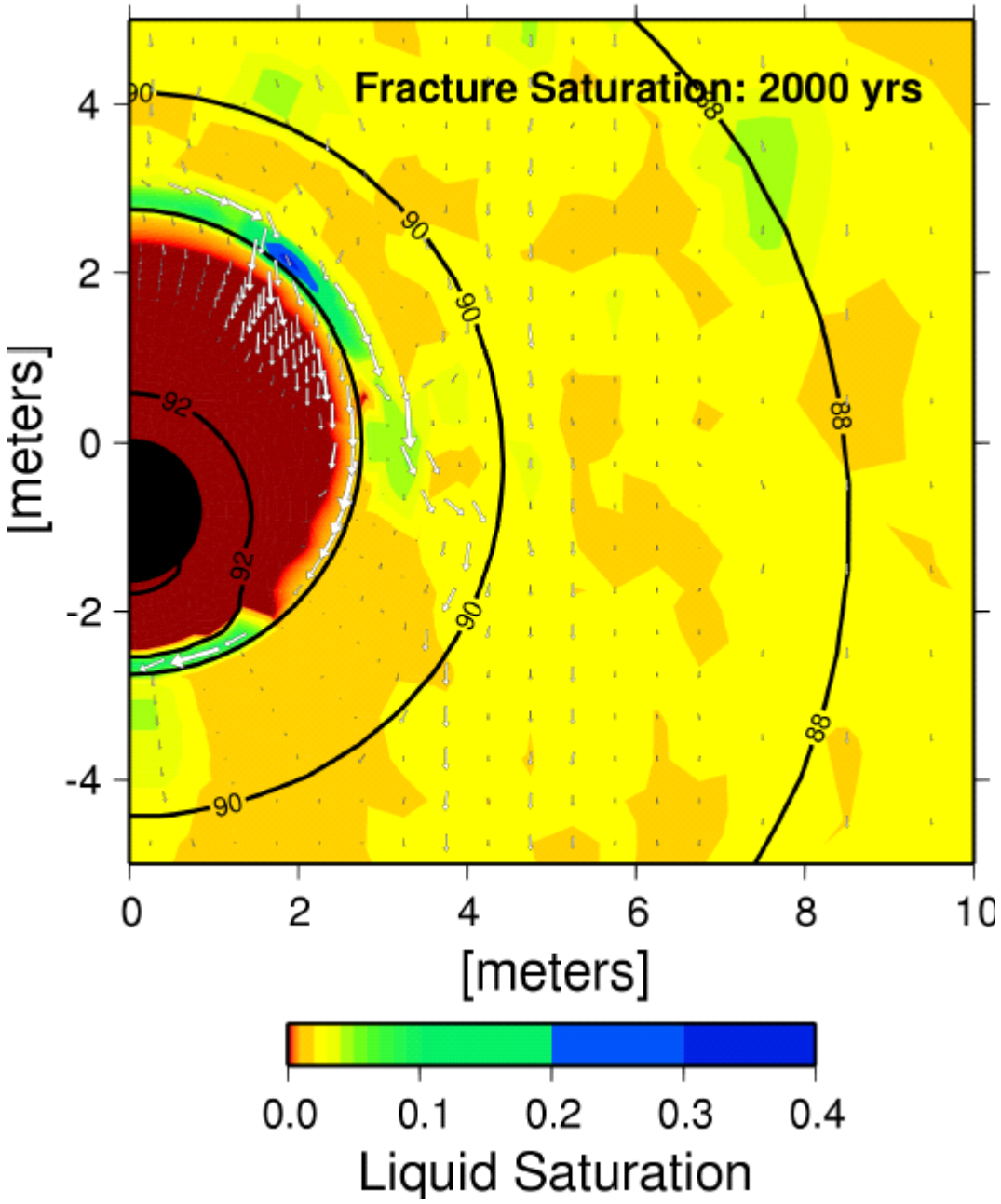

Figure 3b. Contours of saturation and temperature (solid lines), and liquid flux vectors in THC simulations at 2,000 years

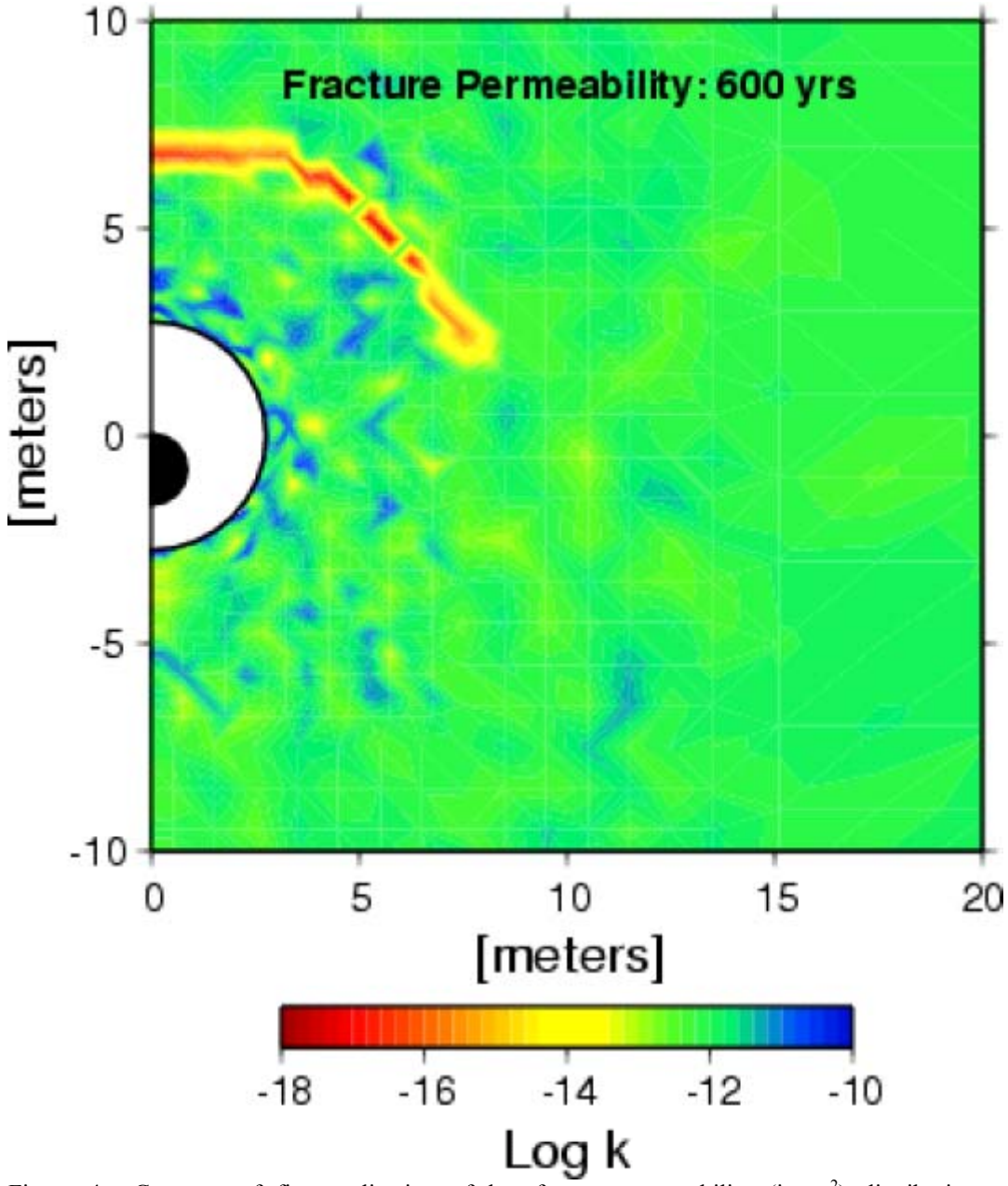

Figure 4a. Contours of first realization of log fracture permeability (in m^2) distribution near the emplacement tunnel at 600 years of THC simulations

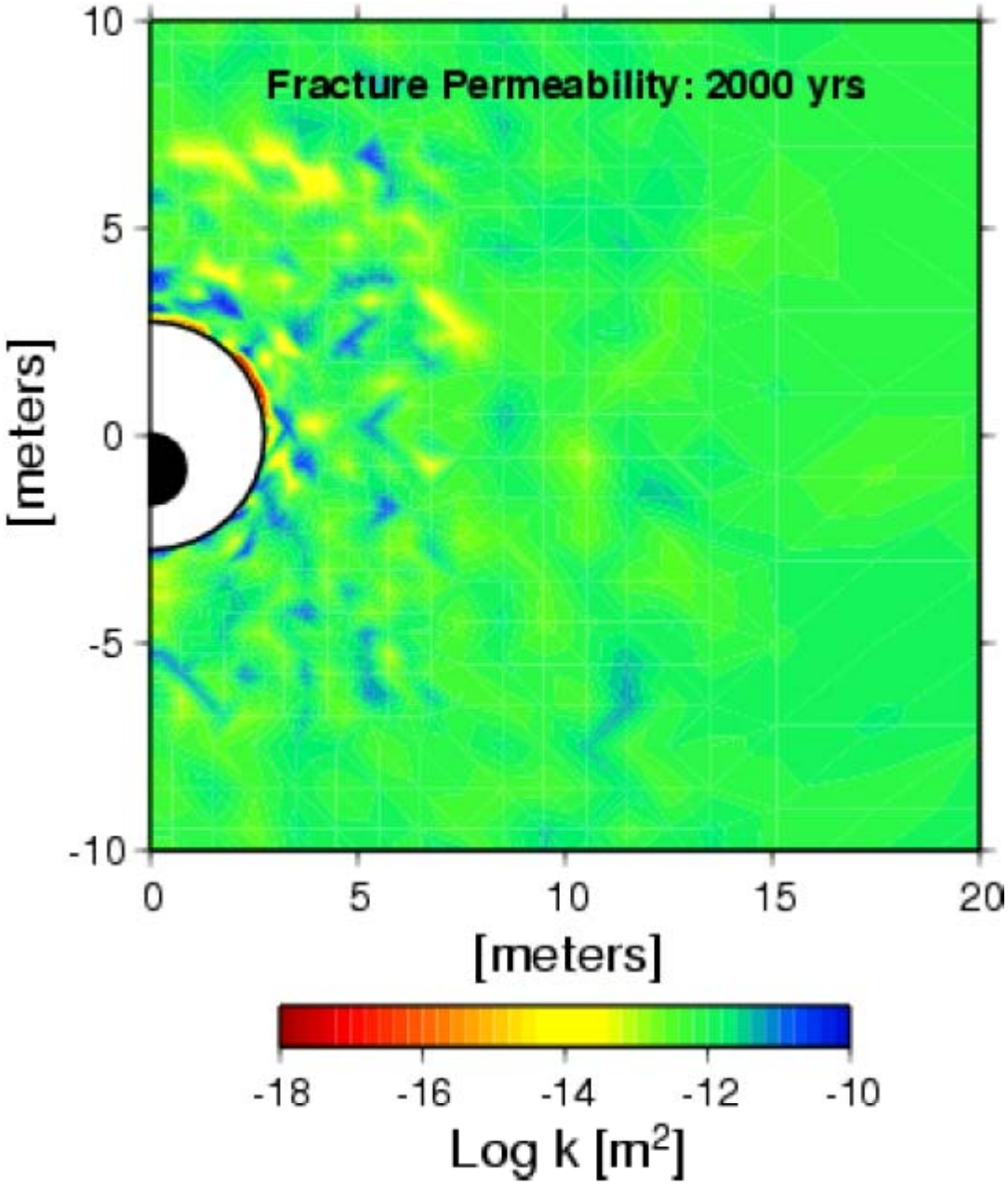

Figure 4b. Contours of first realization of log fracture permeability (in m^2) distribution near the emplacement tunnel at 2,000 years of THC simulations

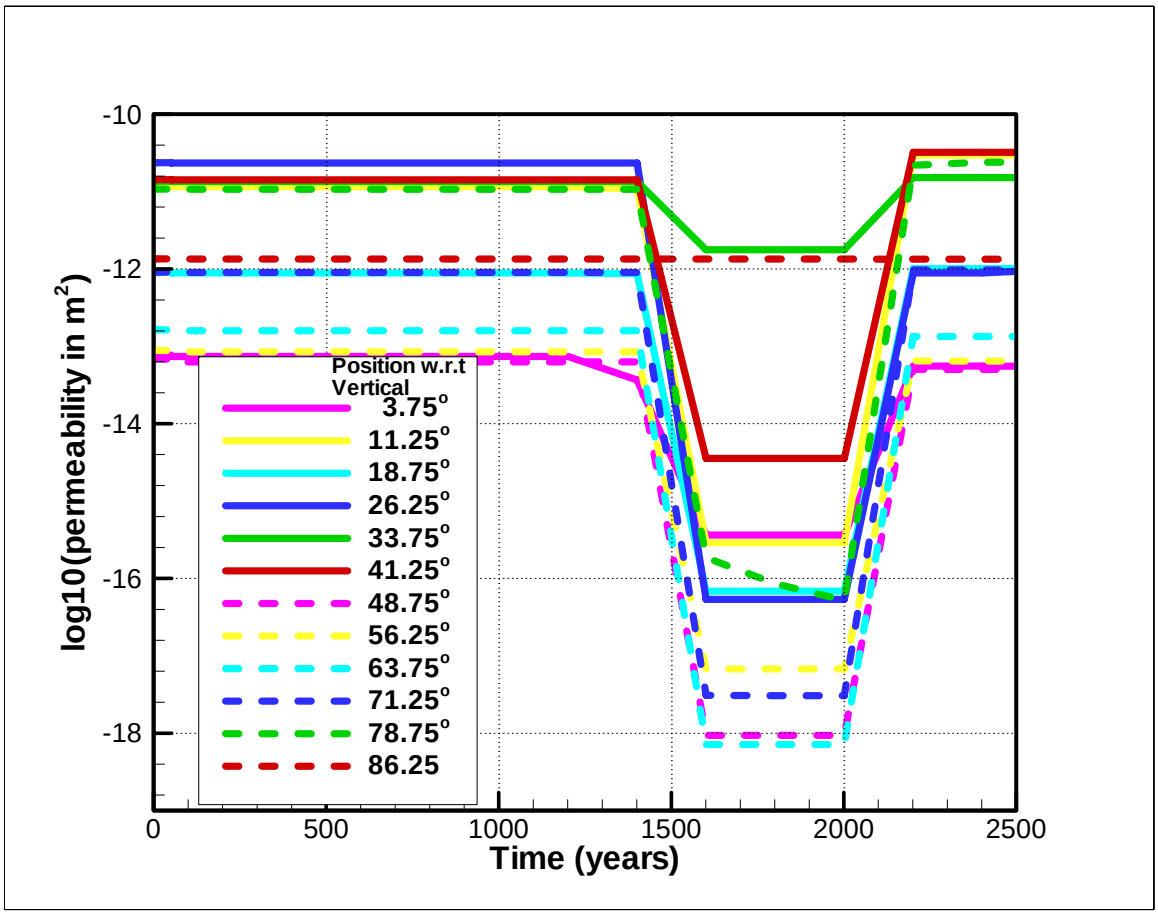

Figure 5. Fracture permeabilities of the grid blocks above the emplacement tunnels as a function of time for THC simulations with the first realization of the fracture permeability field.

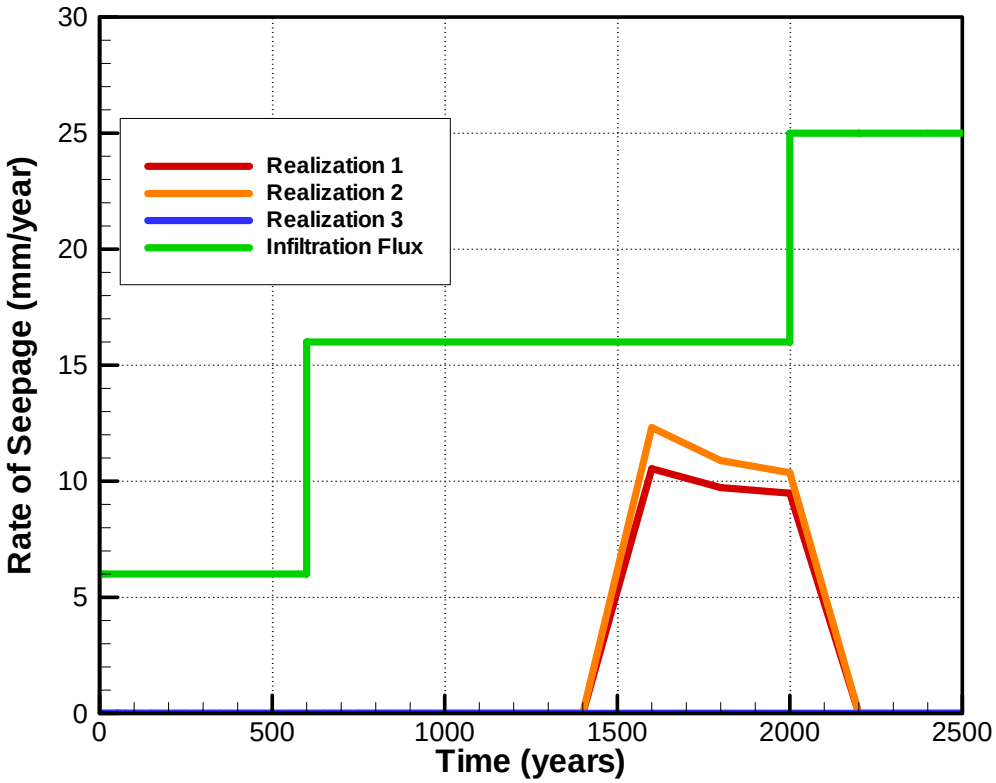

Figure 6. Comparison of rate of seepage into and liquid flow out of the emplacement tunnels from the three different realizations of the fracture permeability distribution. The seepage rates shown are from THC simulations, no seepage takes place in TH simulations.